Chemical Science

ROYAL SOCIETY OF CHEMISTRY

REVIEW

View Article Online
View Journal | View Issue

Cite this: *Chem. Sci.*, 2026, **17**, 1518

Confining chromophores by rigidification of polymer conformation for room-temperature phosphorescence hydrogels

Weihao Feng,[ab] Muqing Si,[ab] Kuangzheng Cao,[c] Wei Lu,[*ab] Xiaoye Zhang*[ab] and Tao Chen[*ab]

Received 31st October 2025
Accepted 23rd December 2025

DOI: 10.1039/d5sc08423g

rsc.li/chemical-science

Organic room-temperature phosphorescence (RTP) materials have played an important part in several emerging photonic applications, such as flexible electronics, bioimaging, and information anti-counterfeiting encryption, due to their large Stokes shift and long lifetime. However, RTP emission of polymer materials requires restriction of a rigid chemical environment, which greatly limits their applications in the dry state, and they usually have poor stretchability. Polymeric RTP hydrogels offer excellent soft, wet features and tunable mechanical properties, providing an ideal solution to address this challenge. Various preparation strategies have been developed to achieve RTP emission by confining chromophores through polymer conformation rigidification, such as physical doping, chemical grafting, and supramolecular polymerization. This review aims to systematically summarize recent progress in this young (but flourishing) research area. Subsequently, the application fields of polymeric RTP hydrogels are reviewed briefly. The current challenges and future outlooks of this field are discussed to attract new interest and inspire more efforts.

1. Introduction

Organic room-temperature phosphorescence (RTP) materials are photoluminescent materials with long emission lifetimes.[1–6] RTP emission can persist after the excitation light stops. Due to a large Stokes shift and long lifetime, RTP materials play an important part in many emerging photonic applications, such as flexible electronics,[7–10] bioimaging,[11–14] and information anti-counterfeiting encryption.[15–18] RTP generation requires electrons to overcome spin prohibition and realize the intersystem crossing of singlet and triplet states. However, triplet excitons are readily quenched by oxygen or return to the ground state through non-radiative transitions.[19,20] Therefore, in order to achieve RTP emission, strategies such as host–guest interactions,[21,22] metal–organic frameworks (MOFs),[23,24] and crystals[25,26] are commonly employed to confine the chromophores in a dry and rigid chemical environment. These approaches reduce the non-radiative decay of the triplet state caused by the movement and collision of phosphorescent molecules and the quenching of triplet excitons by oxygen, and achieve RTP emission. Therefore, most traditional RTP materials often have poor biocompatibility and flexibility, which greatly limits their promotion in practical applications.[27,28] The development of flexible and soft RTP materials has attracted great interest.

Polymeric hydrogels, which usually exist as highly water-swollen quasi-solids and combine many advantages of solution and solid states, have excellent biocompatibility and tunable mechanical properties.[29–34] Combining the superior properties of RTP materials with hydrogels to construct polymeric RTP hydrogels provides an ideal solution to the challenges stated above. Polymeric RTP hydrogels exhibit outstanding flexibility and processability, which enable them to adapt to complex surfaces for applications in wearable devices, flexible sensors and soft robots. Meanwhile, the hydrogel network can respond to external stimuli (*e.g.*, pH, temperature, and specific molecules), resulting in changes in volume or conformation, thereby modulating RTP emission. This property provides a new strategy for anti-counterfeiting and information encryption. In addition, compared with many traditional RTP materials with poor biocompatibility and difficulty in aqueous dispersion, polymeric RTP hydrogels have broad application prospects in bioimaging. Consequently, polymeric RTP hydrogels have numerous irreplaceable advantages over conventional rigid RTP materials. However, polymeric RTP hydrogels are highly sensitive to environmental conditions and readily quenched. The swelling of polymer networks and hydration effect of molecular fragments inevitably enhance polymer chain

[a]*State Key Laboratory of Advanced Marine Materials, Zhejiang Key Laboratory of Extreme-environmental Material Surfaces and Interfaces, Ningbo Institute of Materials Technology and Engineering, Chinese Academy of Sciences, Ningbo 315201, China. E-mail: luwei@nimte.ac.cn; zhangxiaoye@nimte.ac.cn; tao.chen@nimte.ac.cn*

[b]*School of Chemical Sciences, University of Chinese Academy of Sciences, 19A Yuquan Road, Beijing 100049, China*

[c]*Department of Digital Technologies, Hainan Bielefeld University of Applied Sciences, Danzhou 571700, China*

flexibility, resulting in a significant increase in fast non-radiative decay (k_{nr}) or oxygen quenching (k_q).[35] The core idea to solve the problems stated above is to provide a rigid microenvironment for chromophores in hydrogels. "Rigid microenvironment" refers to the rigidification of the chemical environment around chromophores, including molecular-scale (*e.g.*, hydrogen bonds, host–guest interactions, and coordination bonds) or larger-scale (*e.g.*, crystallization and phase separation) interactions. Construction of a rigid microenvironment can stabilize triplet excitons, inhibit non-radiative transitions, and thereby achieve RTP emission.[36–43]

Research on polymeric RTP hydrogels is in its infancy, but several excellent studies have been reported. A review has summarized RTP hydrogels from the perspective of chromophore types,[44] but a review examining RTP hydrogels from the standpoint of preparation strategies is lacking. This review aims to systematically outline the construction of polymer RTP hydrogels and their RTP properties. Polymeric RTP hydrogels are primarily classified into three fabrication strategies: physical doping, chemical grafting and supramolecular polymerization of hydrogels (Scheme 1). Subsequently, a brief introduction is provided to the various potential applications of polymeric RTP hydrogels, including three-dimensional (3D) printing, bioimaging and anti-counterfeiting encryption. Finally, future challenges and prospects are discussed. This review is likely to attract widespread attention from interdisciplinary researchers, providing theoretical guidance and innovative insights for the design and application of next-generation smart materials.

2. Mechanistic insights

2.1 Fundamental mechanism of RTP

RTP arises from a process in which molecules, upon excitation, undergo intersystem crossing (ISC) to reach the triplet state, and then slowly radiate light.[45] The key challenge is that excitons in the delicate triplet state are highly prone to losing energy through non-radiative transitions, such as vibrational and rotational motions, at room temperature, leading to phosphorescence quenching. Therefore, suppressing non-radiative transitions is essential for achieving efficient RTP. The question then becomes: how can we create such a rigid microenvironment in soft, water-rich hydrogels?

2.2 Crucial role of rigid microenvironments in RTP

Hydrogels are macroscopically soft, but their crosslinked network structure at the microscopic level provides effective spatial confinement, or a rigid microenvironment, which is a decisive factor in suppressing non-radiative transitions and regulating RTP lifetime (τ). The crosslinking density of the

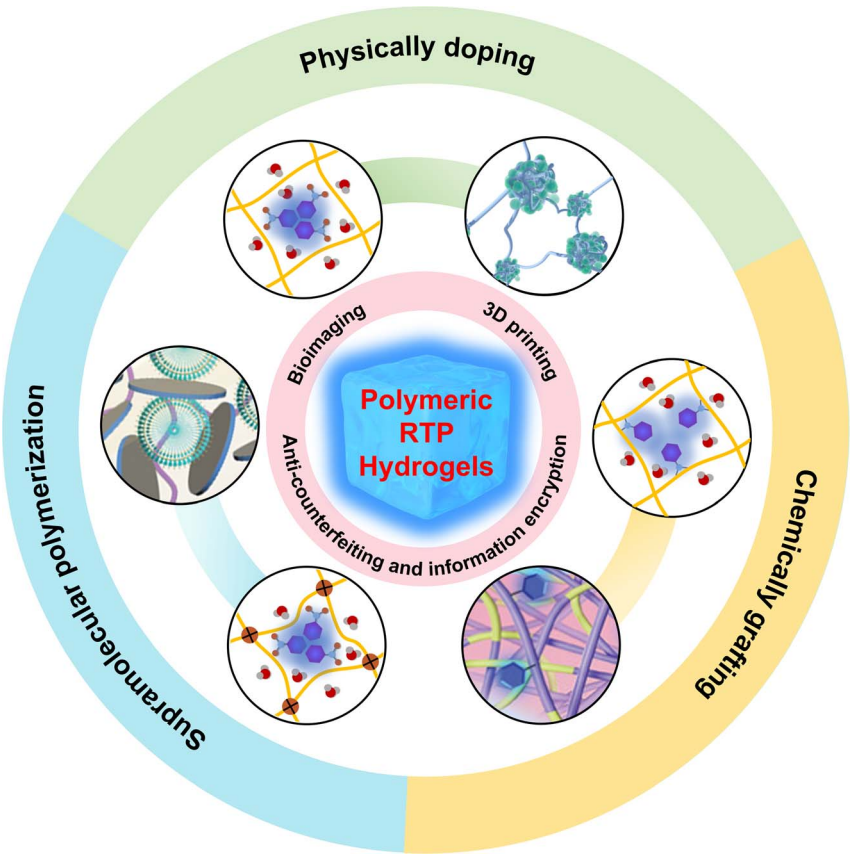

Scheme 1 Synthetic strategy of polymeric RTP hydrogels and their applications in numerous frontier fields.

polymer network influences the RTP intensity of the hydrogel. Studies have shown that, as the polymerization time increases, the RTP intensity gradually improves.[46] The water content is also an important factor influencing RTP performance. Compared with polymer networks with high water content, those with low water content have more densely packed polymer chains, blocking oxygen pathways, and significantly enhancing RTP. Furthermore, introducing rigid segments is a key method to improve RTP. For example, the crystallization within a polyvinyl alcohol (PVA) gel network increases rigidity, reducing the mobility of chromophore molecules and enhancing RTP performance.[47] Incorporation of rigid nanoparticles as multifunctional crosslinking points improves mechanical properties but also creates more restricted "rigid nanodomains" that help stabilize triplet excitons (Fig. 1).[48]

In addition to the adjustment of the polymer network, the interactions between the polymer matrix and chromophore affect RTP performance. For instance, hydrogen bonds between molecules and side-chain amides can limit the mobility of the chromophore but may also alter its electronic structure, thereby facilitating ISC. The spatial confinement of chromophore molecules in an ultra-entangled polymer network, induced by hydrogen bonding, results in ultralong RTP. Moreover, some dynamic crosslinked hydrogels may exhibit reversible changes in RTP performance in response to external stimuli. In summary, this strategy of creating a "rigid microenvironment within a soft matrix" establishes the conditions necessary to stabilize triplet excitons within the macroscopic softness of hydrogels. This forms the foundation for achieving long-lived, high-intensity RTP.

3. Construction strategy of polymeric RTP hydrogels

3.1 Physical doping of chromophores into polymeric hydrogels

Physical doping is the simplest and most direct method for creating polymeric RTP hydrogels. However, phosphorescent chromophores are highly sensitive to the abundant water and dissolved oxygen in hydrogels, readily leading to non-radiative transitions and quenching of triplet excitons. Therefore, chromophores are often protected by encapsulating them within nanoparticles or by utilizing their interactions with polymer matrices.

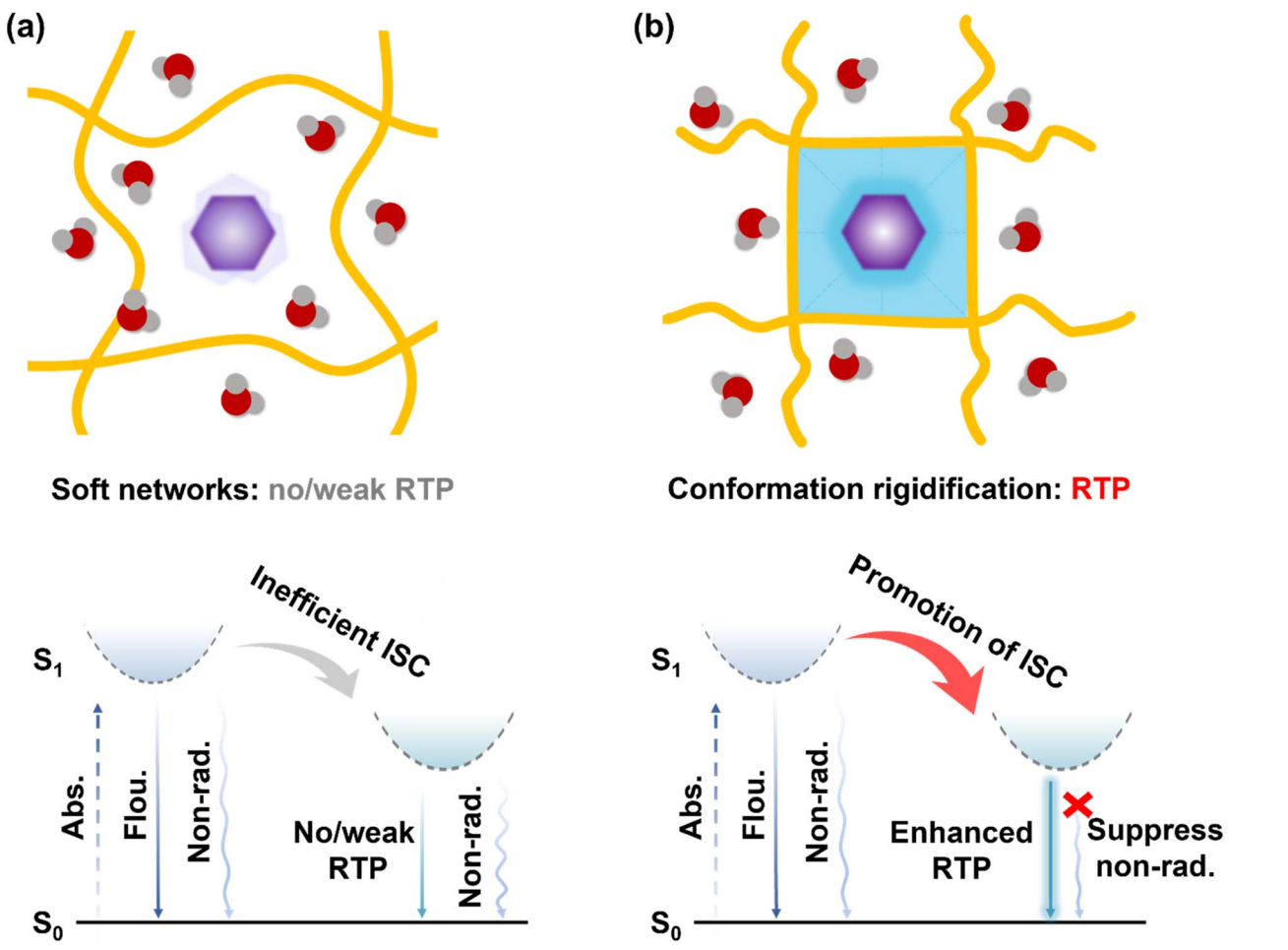

Fig. 1 Mechanism of action of polymeric RTP hydrogels. Schematic Jablonski illustration depicts luminescence mechanisms in (a) soft networks and (b) rigid microenvironments.

The formation of stable nanoparticles through assembly represents an effective method for preparing RTP hydrogels. In 2022, He *et al.* proposed a strategy for the preparation of polymeric RTP hydrogels by boric acid (BA)-doped silicon nanoparticles (BSiNPs). (3-Aminopropyl)trimethoxysilane (APTMS) was reacted with trisodium citrate under microwave irradiation to produce silicon-based nanoparticles (SiNPs), which exhibited blue fluorescence emission. BAs were subsequently doped into the SiNPs system. Glassy-state BSiNPs were formed after a high-temperature and pressure reaction (Fig. 2a).[48] The encapsulated glass-state BSiNPs could stabilize triplet excitons and reduce non-radiative transitions. RTP properties were effectively enhanced. As shown in Fig. 2b, BSiNPs were uniformly dispersed in polyvinyl alcohol (PVA) hydrogels. They exhibited ultralong afterglow up to 20 s (Fig. 2c).

Carbon nanodots (CNDs) enable long-lived phosphorescence. In 2024, Liu *et al.* developed a strategy to achieve phosphorescence emission in hydrogels by encapsulating CNDs within a silica shell, thereby shielding them from water and oxygen. Polymeric RTP hydrogels were then fabricated through *in situ* polymerization with acrylic acid (AA), C=C bond-modified β-cyclodextrin (β-CD-DA) and adamantane (Ad-DA) (Fig. 3a).[49] As shown in Fig. 3b, CNDs@silica were uniformly dispersed in the hydrogels. CNDs@silica provided long-lived green phosphorescence, and the polymeric RTP hydrogels exhibited an ultralong lifetime of up to 1261 ms (Fig. 3c). β-CD-DA and Ad-DA confer >30-times the stretchability to hydrogels through host–guest interactions (Fig. 3d). Furthermore, the hydrogel was able to efficiently transfer energy to the fluorescence dyes rhodamine B and eosin Y through efficient TS-FRET, resulting in long-lived red and yellow delayed fluorescence (Fig. 3a).

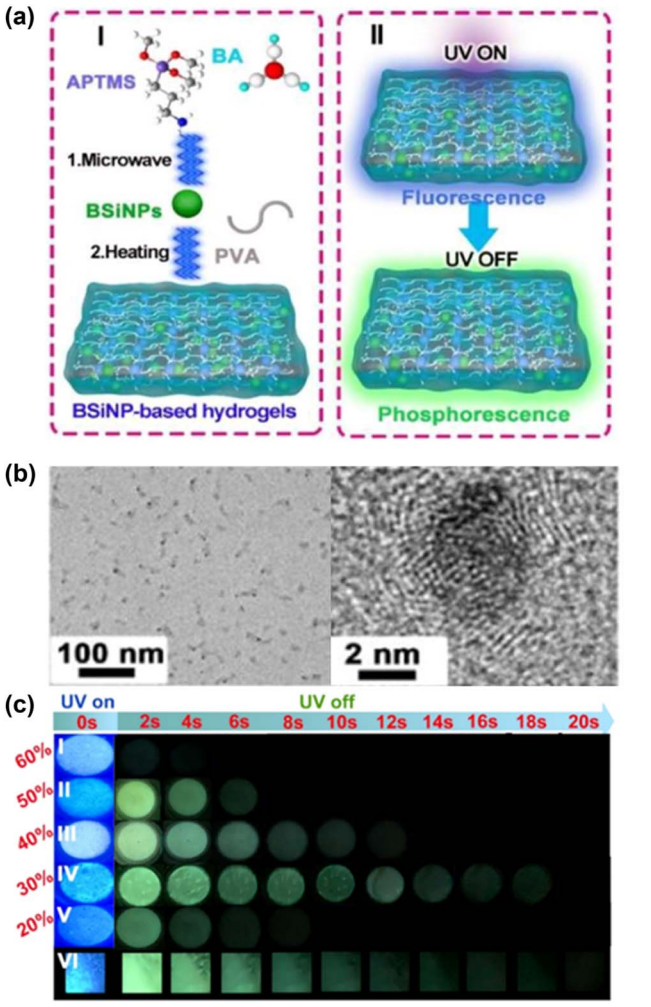

Fig. 2 Physical doping of chromophores into polymeric RTP hydrogels. (a) Synthesis of boron-doped silicon nanoparticles (BSiNPs) and BSiNP-based RTP hydrogels under microwave irradiation. (b) Transmission electron microscopy (TEM) images of BSiNPs. (c) RTP photographs of BSiNPs with different Si/Si + B (mol%) values and hydrogels.

Beyond encapsulating phosphorescent chromophores to shield them from water and oxygen, leveraging physical interactions between chromophores and polymer matrices offers a more universal and direct approach to forming physically doped RTP hydrogels. For example, the hydrogen bonding between chromophores and polymeric chains can effectively achieve RTP emission. In 2025, Wang *et al.* developed a polymeric RTP hydrogel construction method based on strong hydrogen bonding interactions between nonconventional chromophores (NCCs) and polymeric chains (Fig. 4a).[50] Biuret (BIU), polyvinyl alcohol (PVA), and polymaleic acid (PMAc) were dissolved in a glycerol/water mixed solvent and formed organohydrogels (PVA/BIU/PMAc) through freeze–thawing. The strong hydrogen bonds between NCCs and polymer chains suppress non-radiative transitions and promote the aggregation of NCCs, thereby stiffening molecular conformations and forming spatial conjugation. RTP hydrogels exhibited an RTP lifetime of up to 782.8 ms (Fig. 4b). Furthermore, the hydrogels demonstrated significant excitation-dependent RTP emission. Remarkably, the RTP emission wavelength of the hydrogels varied with the change in the excitation wavelength (Fig. 4c).

By forming hydrogen bond interactions between the polymer chains and chromophores, not only can polymeric RTP hydrogels be constructed, but the hydrogels are also endowed with excellent mechanical properties. In 2024, Chen *et al.* developed high-strength polymeric RTP hydrogels (W-hydrogels) by the *in situ* polymerization of acrylamide (AAm) in the presence of delignified wood. This strategy aimed to form molecular clusters through hydrogen bond interactions between lignin and acrylamide (Fig. 4d).[51] Such enhanced interactions facilitate the confinement of lignin and trigger the radiative migration of triplet excitons, thus enabling RTP emission. The hydrogels exhibited RTP emission at ~490 nm and gave out obvious green luminescence after removing UV light (Fig. 4e). As a result of the molecular interactions between the components of delignified wood and polyacrylamide (PAAm), the W-hydrogels exhibited extremely high tensile strength. Moreover, the tensile strength of W-hydrogel treated with ethanol increased significantly, and the entire process was reversible (Fig. 4f). The reversibility of this process enables the RPT hydrogel material to be applied in a wide range of scenarios.

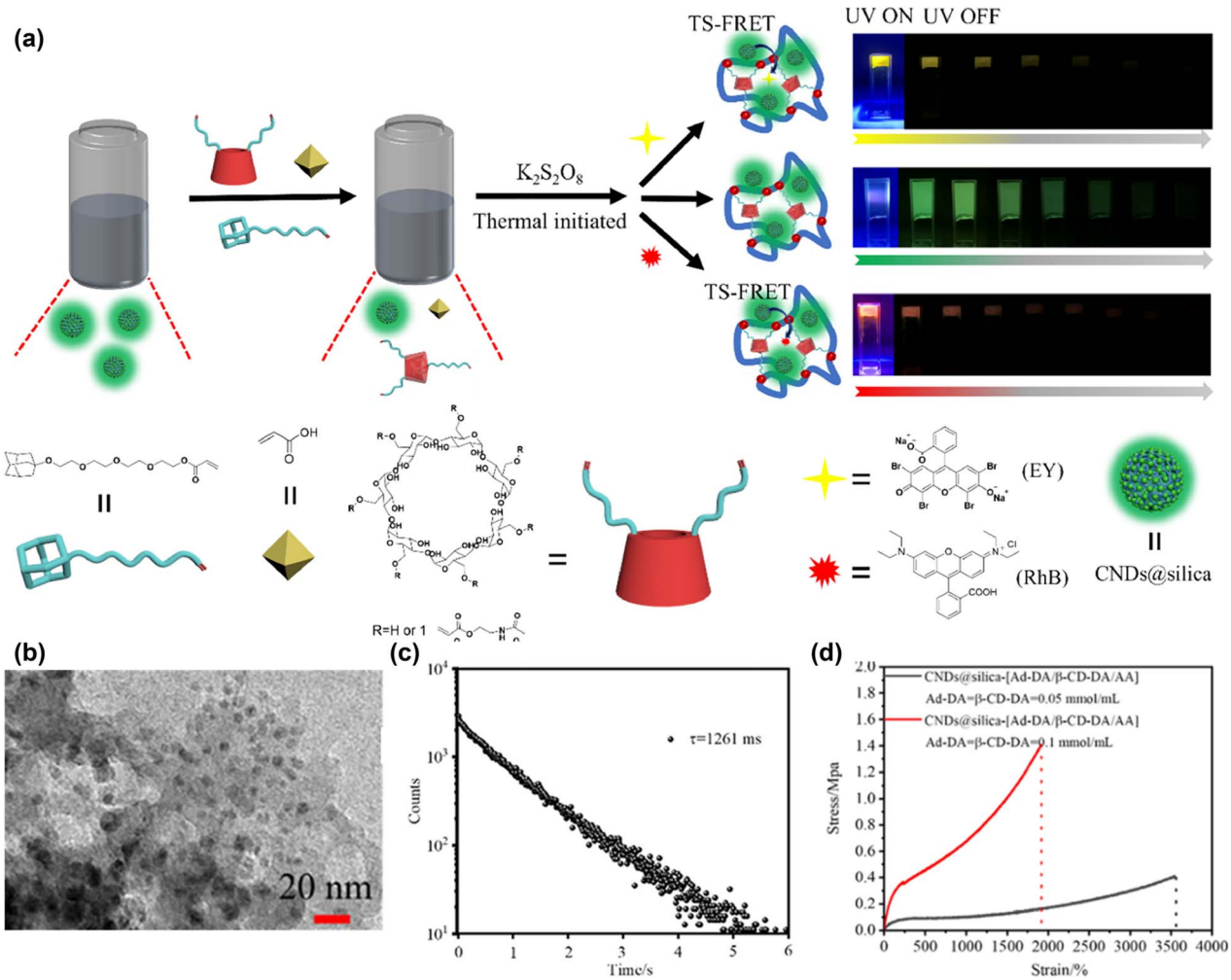

Fig. 3 Physical doping of chromophores into polymeric RTP hydrogels. (a) Construction of CNDs@silica-(Ad-DA/β-CD-DA/AA) hydrogels and the green RTP and delay fluorescence photographs of hydrogels. (b) TEM images of CNDs@silica. (c) Lifetime decay curve of a hydrogel collected at 520 nm. (d) Tensile stress–strain curves of hydrogels with different concentrations of Ad-DA/β-CD-DA assembly.

These chromophores interact with polymer chains to form a super-entangled state, enabling the hydrogel to effectively achieve phosphorescent emission and super-stretch properties. In 2025, Chen *et al.* incorporated 4-diphenylboronic acid@β-Cyclodextrin (4-BB@β-CD) into a poly(2-(acryloxy)ethyl trimethylammonium chloride) (PAETC) network to prepare an ultra-stretchable polymer RTP hydrogel. Under water-limiting conditions, the PAETC chain forms a hyper-entangled structure and synergistically densifies the 4-BB@β-CD aggregates through supramolecular confinement, effectively suppressing molecular vibrations and stabilizing triplet states (Fig. 5a).[52] Impressively, the hydrogels exhibit intense RTP emission at ~500 nm and ultralong lifetime up to 970.7 ms under room conditions (Fig. 5b and c). Crucially, the entanglement-dominated physical network free of static chemical cross-linking enables continuing chain disentanglement during stretching for efficient energy dissipation, achieving excellent uniaxial/biaxial (21 000%/10 000%) stretchability (Fig. 5d and e). Notably, these PAETC/4-BB@β-CD hydrogels maintained bright and long-lived RTP under various strains (Fig. 5e).

All these impressive recent advancements suggest that excellent and multifunctional RTP properties can be imparted to hydrogel materials through simple physical doping as well as material design.

3.2 Chemical grafting of chromophores into polymeric hydrogels

Physical doping is simple, but the problem of phosphorescent small-molecule leakage significantly limits the long-term stability and practical applications of polymeric RTP hydrogels. To fundamentally address this problem, researchers have covalently grafted chromophores onto the three-dimensional network of hydrogels. Due to the stability of covalent bonds, grafting chromophores onto polymer chains enhances the stability of luminescence intensity and lifetime.[51] Interactions within polymeric networks provide a highly rigid microenvironment for the phosphorescence of chromophores, effectively stabilizing triplet excitons and suppressing non-radiative

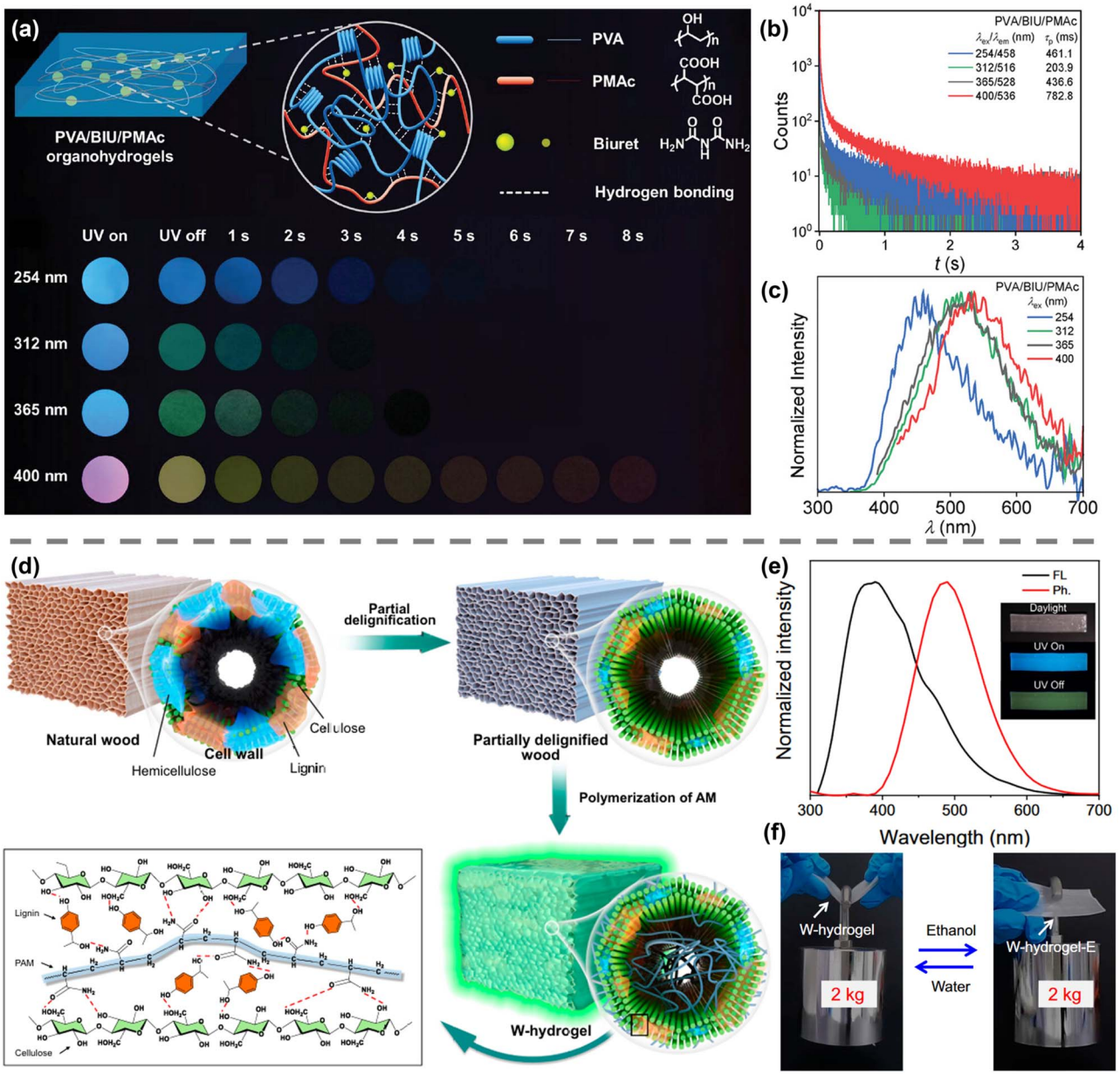

Fig. 4 Physical doping of chromophores into polymeric RTP hydrogels. (a) Crosslinking mechanism in PVA/BIU/PMAc organohydrogels and RTP photographs of hydrogels after ceasing irradiation at different wavelengths (schematic). (b and c) Phosphorescence lifetime profiles and delayed emission spectra of PVA/BIU/PMAc organohydrogels. (d) Preparation of a RTP W-hydrogel from natural wood (schematic). (e) Fluorescence (black line) and phosphorescence spectra (red line) of W-hydrogel upon excitation at 290 nm. Inset: Photographs of a W-hydrogel under visible light, under UV light, and after removing UV light. (f) Photographs of a W-hydrogel and W-hydrogel-E loaded with a weight.

transitions, ultimately facilitating the construction of polymer RTP hydrogels.

For example, formation of a rigid microenvironment through host–guest interactions can enable the preparation of polymeric RTP hydrogels by grafting host and guest molecules onto the polymeric main chain. In 2014, Tian *et al.* grafted β-cyclodextrin (β-CD) and α-bromonaphthalene (α-BrNp) onto the polymeric main chain (Fig. 6a).[53] The host–guest recognition between β-CD and α-BrNp enabled hydrogel formation without the need for additional crosslinking. The rigid microenvironment provided by the host–guest interactions achieved RTP emission and exhibited a lifetime of 0.56 ms. Simultaneously, the hydrogels exhibited excellent self-healing properties (Fig. 6b). Similarly, in 2016, they achieved RTP emission in hydrogels with a lifetime of 0.32 ms by using different host molecule γ-cyclodextrin (γ-CD) and guest molecule 4-bromo-1,8-naphthalic anhydride (BrNpA) (Fig. 6c).[54]

Designing the molecular structure and multi-functionalization of phosphorescent molecules can enable the construction of a rigid microenvironment in hydrogels. In 2024, He *et al.* developed a novel multifunctional molecule based on benzothiadiazole-based dialkene (BTD-HEA), which serves as

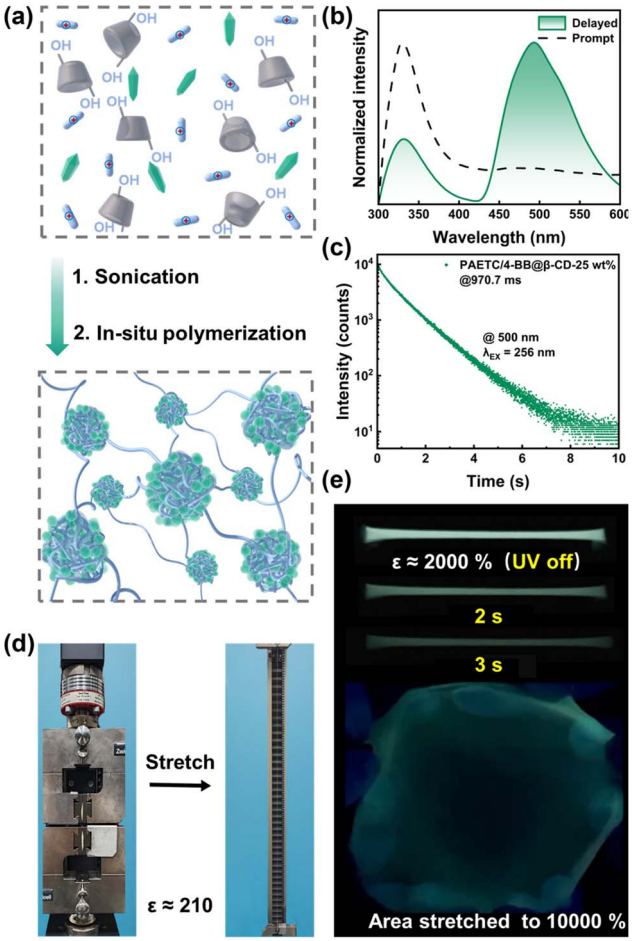

Fig. 5 Physical doping of chromophores into polymeric RTP hydrogels. (a) Synthesis of PAETC/4-BB@β-CD hydrogels. (b) Normalized delayed and prompt luminescence spectrum of PAETC/4-BB@β-CD hydrogels. (c) Time-resolved emission-decay test of the PAETC/4-BB@β-CD-25 wt% hydrogel recorded at 500 nm. (d) Photographs of the PAETC/4-BB@β-CD-25 wt% hydrogel after being stretched by 21 000%. (e) Photographs of the PAETC/4-BB@β-CD-25 wt% hydrogel after uniaxial stretching to 2000% and biaxial stretching to an area strain of 10 000% after removal of UV light.

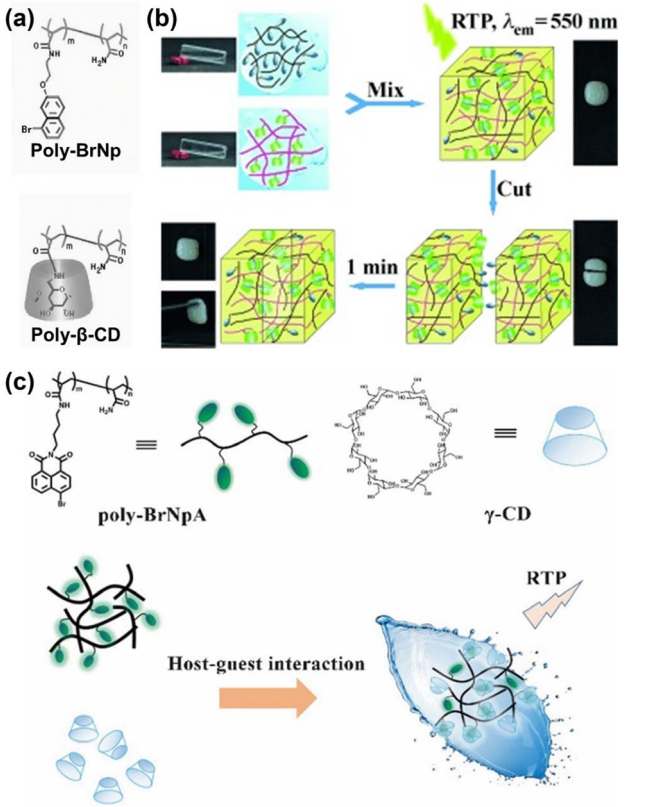

Fig. 6 Chemical grafting of chromophores into polymeric RTP hydrogels. (a) Structures of host polymer poly-b-CD and guest polymers poly-BrNp. (b) Preparation of poly-α-BrNp/poly-β-CD hydrogels and self-healing processes. (c) Polymeric RTP hydrogel *via* host–guest interaction between poly-BrNpA and γ-CD.

a phosphorescence emitter, initiator, and crosslinker in polymeric RTP hydrogels. BTD-HEA exhibits high triplet exciton generation and a dialkene structure, enabling it to effectively initiate the polymerization of acrylamide-based monomers while acting as a site to form a crosslinked network structure (Fig. 7a).[46] Additionally, the distinct fluorescent-phosphorescent colorimetric characteristics of the hydrogel offer a more sensitive approach for visually monitoring polymerization (Fig. 7b). RTP intensity and rheological tests demonstrate that the crosslinking degree of the hydrogel network increases with polymerization time (Fig. 7c and d). Consequently, the thermal motion of BTD-HEA was restricted, and non-radiative transitions were suppressed, leading to changes in RTP emission. By utilizing BTD-HEA as a photoinitiator, various shapes of polyhydroxyethyl acrylate (PHEA) hydrogels can be prepared through 3D printing. Moreover, the hydrogel retains a purple afterglow even after the cessation of 365-nm UV excitation (Fig. 7e). Although purple afterglow is uncommon, its long-lasting luminescence characteristics confirm its RTP emission.

Formation of a phase-separated structure in hydrogels can also achieve the construction of a rigid microenvironment. In 2024, Lü *et al.* induced *in situ* phase separation in hydrogels *via* acid treatment, thereby preparing polymeric RTP hydrogels. Initially, the researchers prepared hydrogels by copolymerizing AAm and *N*-(4-(9H-carbazole-9-yl)phenyl)-2-acrylamide chromophore (CzPA). The hydrogels were then immersed in aqueous hydrochloric acid to hydrolyze the amide groups. The interaction between amide and carboxylic acid groups formed dense hydrogen bonds, leading to phase separation. This process resulted in the formation of a tight network structure that restricted the motion of chromophores and suppressed non-radiative transitions (Fig. 7f).[55] The hydrogels displayed excellent stability in water, showing minimal change over 30 days, with consistent RTP intensity and afterglow (Fig. 7g and h). Mechanical properties play a very important part in expanding the application range of polymeric RTP hydrogels and extending the service life of materials. However, the emission of RTP requires the suppression of non-radiative transitions, which is contradictory to the softness, high water content, and stretchable properties of hydrogels. Therefore, it is

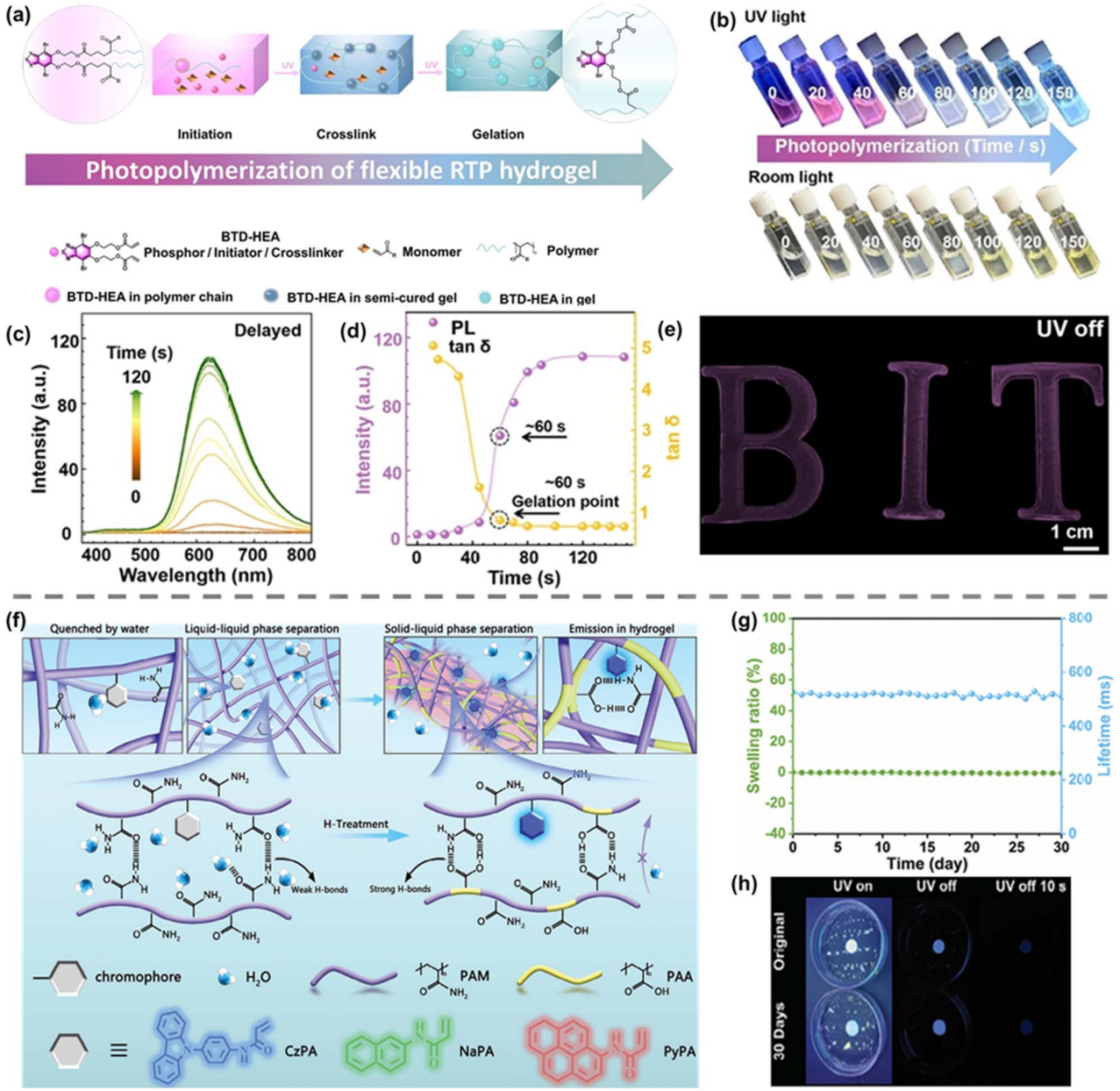

Fig. 7 Chemical grafting of chromophores into polymeric RTP hydrogels. (a) The multifunctional phosphorescent compound of BTD-HEA initiates polymerization to generate a gel. (b and c) Photographs and delayed emission spectra intensity of BTD-HEA with AAm (3 wt%), captured at various stages during gelation under 365-nm UV light. (d) Delayed emission spectra intensity and loss factors of the gelation system with time. (e) Photographs of PHEA hydrogels' phosphorescence emission after deactivating the UV-365-nm excitation source. (f) Mechanism of H-CzPA-co-PAM hydrogels induced by *in situ* phase separation. This process prevents the non-radiative transition of the chromophore, allowing sustainable underwater emission. (g) Swelling ratio and phosphorescence lifetime of H-$CzPA_{0.10\%}$-co-PAM hydrogel with 9 h of H-treatment after placement in water for 30 days. (h) Afterglow photographs of the original H-$CzPA_{0.10\%}$-co-PAM hydrogel with 9 h of H-treatment in water and after immersing in water for 30 days.

necessary to construct a local rigid microenvironment in the hydrogels. Construction of rigid microenvironments does not compromise the overall mechanical properties of the hydrogel, so polymeric RTP hydrogels have the advantage of widely adjustable mechanical properties. In addition to excellent RTP properties, polymeric RTP hydrogels have excellent and widely tunable mechanical properties. In a series of hydrogels with different H-treatment times, the hydrogel treated for 6 h exhibits a fracture strain of nearly 1000%, while the hydrogel treated for 14 h shows a fracture stress of >11 MPa.

In addition to introducing typical chromophores, RTP emission can be achieved by the aggregation and confinement of electron-rich groups, such as carbonyl groups. In 2024, Wu *et al.* proposed a strategy for the preparation of polymeric RTP hydrogels through polymerization-induced crystallization (Fig. 8a).[56] This strategy exploited the solubility difference of

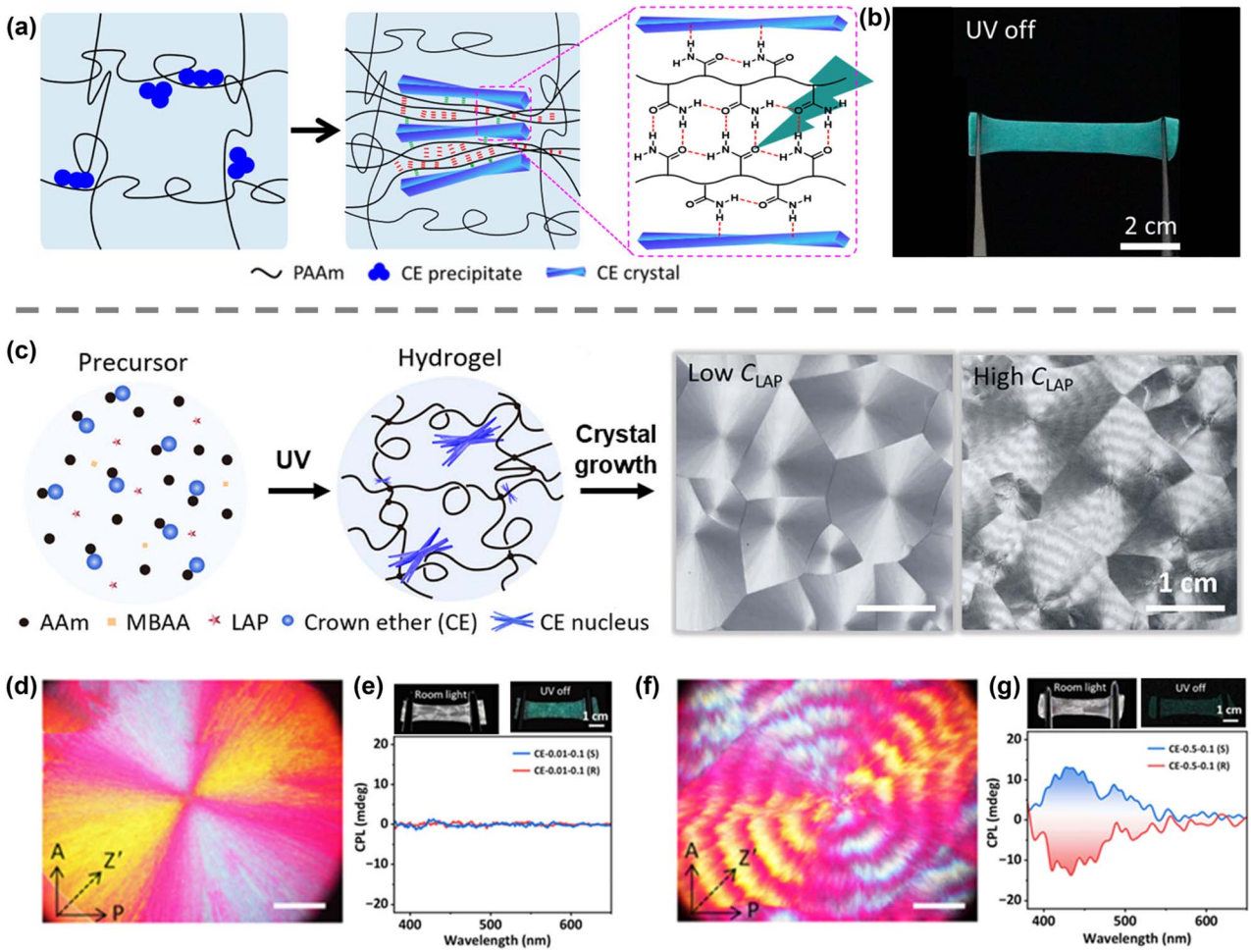

Fig. 8 Chemical grafting of chromophores into polymeric RTP hydrogels. (a) Polymerization-induced crystallization of dopant molecules to form crystals that squeeze and confine the polymeric matrix as cluster phosphors of the composite hydrogel. (b) Photographs of a CE-PAAm gel after being stretched to a strain of 100% after turning off 280-nm UV light. (c) Photopolymerization-induced crystallization of dopant molecules to form different spherulites in CE hydrogels and photographs of composite hydrogels synthesized with low and high initiator LAP concentrations taken under room light, respectively. (d) Polarized optical micrographs of regular spherulites in CE-0.01-0.1 gel. (e) Photographs showing the stretchability of CE-0.01-0.1 gels under room light and turning off the 280-nm UV light. Corresponding CPL spectra of gels with D/L-methionine excited at 280 nm are shown below. (f) Polarized optical micrographs of banded spherulites in CE-0.5–0.1 gel. (g) Photographs showing the stretchability of CE-0.5–0.1 gels under room light and turning off the 280-nm UV light. Corresponding CPL spectra of gels with D/L-methionine excited at 280 nm are shown below.

crown ethers (CEs) in monomer and polymer states. During polymerization, the solubility of the CEs sharply decreases, leading to the formation of large spherulites that compress and confine the polyacrylamide hydrogel matrix. The approach leads to the formation and aggregation of carbonyl group clusters, thereby achieving RTP emission. The hydrogels exhibit excellent stretchability and resilience, with visible afterglow (Fig. 8b).

Building on the research findings stated above, in 2024, Wu *et al.* achieved control of spherulite structure in hydrogels by modulating the hydrogel network stiffness. The stiffness of the PAAm network was precisely adjusted by regulating the concentrations of photoinitiator and chemical crosslinking agents, as well as the intensity of UV light. Regular spherulites are formed in relatively stiff hydrogels, whereas banded spherulites with twisted crystal fibers are obtained in hydrogels (Fig. 8c).[57] The structure of the spherulites can be directly observed through polarized optical microscopy (Fig. 8d and f). The formation of twisted crystalline fibers was linked to the dynamic changes in crystallization pressure and network impedance. Hydrogels with regular spherulites exhibited stronger fluorescence and phosphorescence compared with those with banded spherulites. Surprisingly, the hydrogels with banded spherulites exhibited circularly polarized luminescence (CPL) (Fig. 8e and g). This luminescence arises from the aggregation of clusters constrained by the crystal, while the twisted crystalline fibers give the achiral luminescent clusters CPL. In addition to crystallization-induced carbonyl groups clustering in polymers, the aggregation of carbonyl groups can also be achieved through salt-induced aggregation. In 2024, Zhao *et al.* proposed a new strategy for constructing polymeric RTP hydrogels *via* salt-induced aggregation. AA and diethylenetriamine (DETA) were copolymerized to prepare

a polymer network, which was then immersed in a sodium bromide solution.[58] The salt treatment promotes hydrophobic aggregation in the hydrogel network. The resulting dense structure enabled the clustering of carboxyl groups and oxygen atoms, suppressing non-radiative transitions and thereby enabling RTP emission.

However, despite this impressive progress, the development of polymeric RTP hydrogels is largely lagging, partially because of the tedious synthetic procedures. More efforts are suggested to explore new and simple synthetic methods or the employment of well-organized supramolecular interactions to construct powerful polymeric RTP hydrogels.

3.3 Polymeric RTP hydrogels *via* supramolecular polymerization

Polymeric RTP hydrogels can also be constructed through the spontaneous self-assembly process of supramolecular polymerization of phosphorescence molecules and copolymer monomer molecules. The rigid microenvironment in hydrogels can be constructed through the process of supramolecular self-assembly, enabling RTP emission. Supramolecular polymerization is usually driven by electrostatic interactions, hydrogen bonds, and dipole–dipole interactions. Compared with physically doped polymeric hydrogels and chemically crosslinked polymeric hydrogel systems, supramolecular interactions exhibit high dynamism and reversibility, showing great application potential.

Electrostatic interactions are typical supramolecular interactions between ions with opposite charges (*e.g.*, cations such as quaternary ammonium groups or protonated amino groups and anions such as carboxylate or sulfate groups). Supramolecular interaction sites are formed by the interaction between chromophores and a group with the opposite charge, and the polymeric RTP hydrogel can be prepared by supramolecular polymerization/crosslinking based on electrostatic interaction. For example, in 2021, Garain *et al.* synthesized a simple heavy atom-substituted cationic phthalimide derivative (CPthBr). After that, the researchers used an organic–inorganic supramolecular scaffolding strategy to form supramolecular action sites through the electrostatic interactions between CPthBr and negatively charged LAPONITE® (LP) clays (Fig. 9a).[59] As LP was continuously added to the aqueous solution of CPthBr, an RTP emission peak ~487 nm was continuously enhanced (Fig. 9b). The phosphorescence lifetime was 1.62 ms (Fig. 9c). At higher LP concentrations, the LP scaffold promoted the orderly arrangement of molecules through electrostatic interactions to form unique self-standing supramolecular RTP hydrogels. Efficient triplet-to-singlet FÖrster resonance energy transfer and delayed fluorescence were achieved by doping Sulforhodamine G (SRG) and Sulforhodamine101 (SR101) dyes into CPthBr-LP hydrogels. Yellow and orange RTP hydrogels can be produced with average lifetimes of 162 μs and 55 μs, respectively (Fig. 9d).

Hydrogen bonds are also important supramolecular interactions for constructing supramolecular polymeric RTP hydrogels. Usually, a single hydrogen bond is too weak to stabilize supramolecular materials, but the synergistic effect of hydrogen bonds and other supramolecular interactions is conducive to the preparation of supramolecular polymeric hydrogels. For example, in 2024, Dai *et al.* developed near-infrared (NIR) RTP supramolecular hydrogels based on amphiphilic bromonaphthalimide pyridinium derivative (G), LP nanosheets and PAAm. Initially, G molecules can self-assemble into positively charged spherical nanoparticles without RTP properties. Driven by electrostatic interactions, these nanoparticles can be co-assembled with negatively charged LP to form supramolecular RTP hydrogels (Fig. 9e).[60] This hydrogel exhibits red RTP phosphorescence at 586 nm with a lifetime of 4.03 ms. Furthermore, the physical crosslinking network is enhanced by introducing PAAm into the supramolecular RTP hydrogel system. The abundant hydrogen bonding intensifies RTP intensity and improves lifetime to 4.20 ms (Fig. 9f and g). In particular, RTP emission can be achieved at a higher temperature (363 K) with a lifetime of 2.46 ms (Fig. 9h and i).

Similarly, in 2025, Dai *et al.* prepared supramolecular polymeric RTP hydrogels based on electrostatic interactions and hydrogen bonding synergy through green one-pot copolymerization of monoalkene-functionalized iodoisoquinolinium derivatives (G′), LP, and AAm monomers in aqueous solution (Fig. 9j).[61] This approach circumvents the multi-step assembly procedures employed in previous studies, thereby facilitating the construction of supramolecular polymeric RTP hydrogels.

Dipole–dipole interactions play an important part in supramolecular polymerization. By rationally designing the polar groups in molecules, the molecules can be induced to self-assemble into nanoscale structural units and then be polymerized into hydrogels. Formation of these supramolecular polymeric hydrogels typically relies on dipole–dipole interactions, but also on other types of supramolecular interactions. For example, in 2023, Xiao *et al.* designed supramolecular polymeric RTP hydrogels prepared by simply heating/mixing and cooling hexamethyl cucurbit[5]uril (HmeQ[5]) and 1,4-diaminobenzene (DB).[62] HmeQ[5] has two ports surrounded by carbonyl groups. The dipole–dipole interaction and hydrogen bonding between HmeQ[5] and the amino group of protonated DB played an important part in supramolecular polymerization. Scanning electron microscopy (SEM) showed the morphology of the freeze-dried hydrogel, exhibiting a fiber network structure. The incorporation of chromophores induces stimulated RTP emission in the ordered fiber structure of the supramolecular hydrogel, effectively suppressing non-radiative transitions. This effect can be proved by confocal laser scanning microscopy. Meanwhile, due to the temperature sensitivity of the supramolecular interactions, a sol-to-gel transition was observed when the hydrogels were cooled to 25 °C, while a gel-to-sol transition was observed at 75 °C.

4. Applications of polymeric RTP hydrogels

Polymeric RTP hydrogels, as a new generation of intelligent materials, hold immense application potential due to their outstanding biocompatibility, flexible and stretchable mechanical properties, as well as a three-dimensional porous

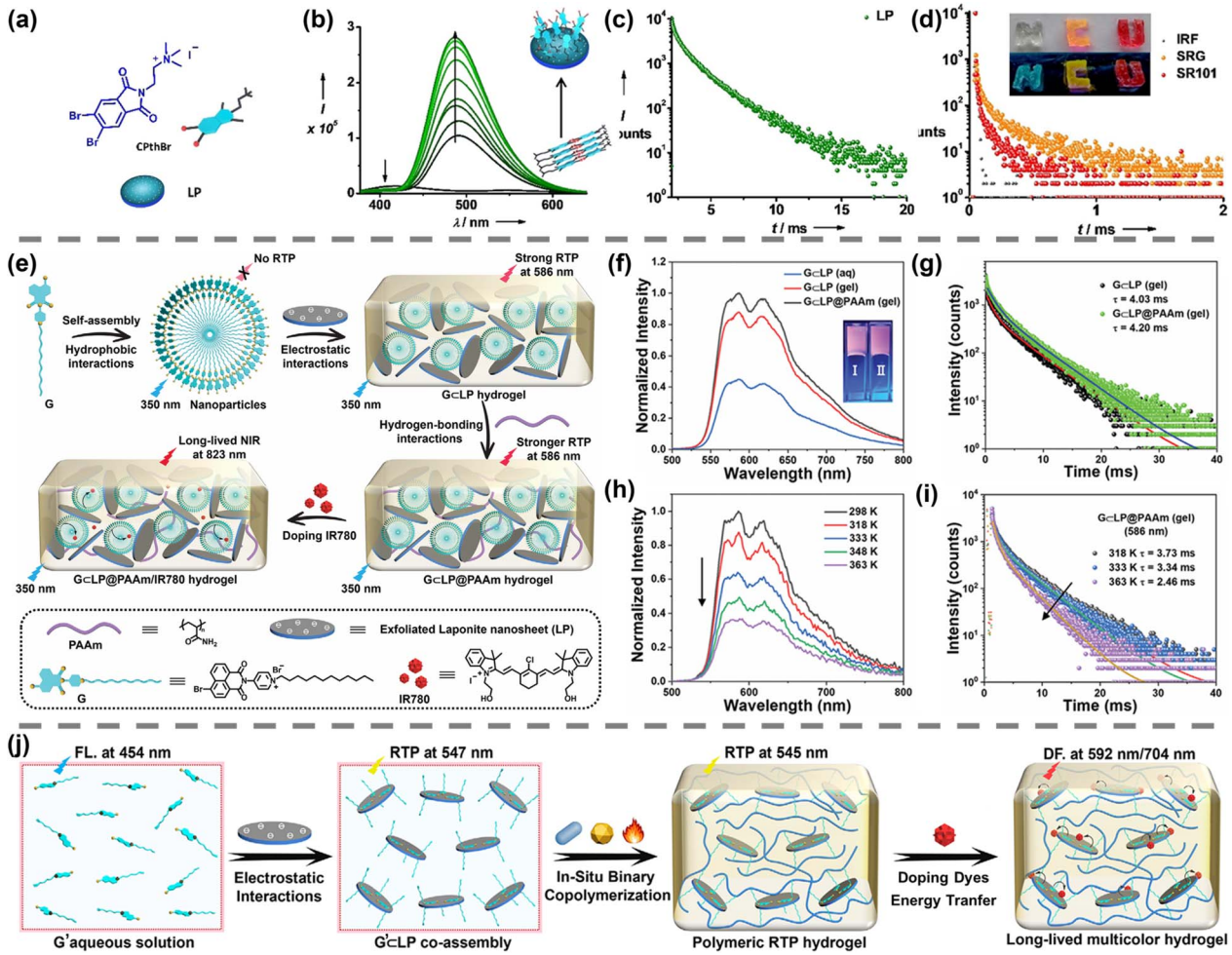

Fig. 9 Polymeric RTP hydrogels *via* supramolecular polymerization. (a) Molecular structure and schematic representation of CPthBr and LP. (b) Photoluminescence titration study of CPthBr with increasing the LP wt% (0.125 wt% to 6 wt%) in an aqueous solution. (c) Lifetime decay plot of a CPthBr-LP hybrid. (d) Delayed fluorescence lifetime decay plot of 10 : 1 CPthBrSRG-LP and CPthBr-SR101-LP hybrid hydrogels. Inset: photographs of self-standing hydrogel and "NCU" is written under visible light and under 254-nm UV light using a hydrogel. (e) Preparation of NIR G⊂LP@PAAm hydrogels based on amphiphilic bromonaphthalimide pyridinium hierarchical assembly. (f) Phosphorescence emission spectra of G⊂LP (aq), G⊂LP hydrogel and G⊂LP@PAAm hydrogel. (g) Time-resolved photoluminescence decay spectra of G⊂LP hydrogel and G⊂LP@PAAm hydrogel at 410 nm. (h) Normalized phosphorescence emission spectra of G⊂LP@PAAm hydrogel at different temperatures. (i) Time-resolved photoluminescence decay spectra of G⊂LP@PAAm hydrogel at 318, 333, and 363 K. (j) Construction of robust G′⊂LP@PAAm hydrogels *via* green *in situ* copolymerization in aqueous solution (schematic).

network.[63–68] In terms of optical performance, their unique long-term stability, tunability, and stimulus-responsive luminescence characteristics make them highly promising for applications in 3D printing, bioimaging, and complex information encryption technologies. This section will briefly summarize the application progress of RTP hydrogels in these fields.

4.1 3D printing

Polymeric RTP hydrogels have the advantages of long lifetime, non-interference background and easy preparation into 3D shapes.[69,70] Polymeric RTP hydrogels have been processed into 3D shapes with distinct luminescence (Fig. 10a).[51] Subsequently, these hydrogels were fabricated into micron-sized hydrogel threads and applied to the suture of biological tissues (Fig. 10b and c). However, hydrogels prepared using the template method exhibit low precision, making it challenging to fabricate polymeric RTP hydrogels with complex 3D macroscopic structures (*e.g.*, porous scaffolds). 3D printing technology offers advantages in forming complex structures and achieving high precision. Photo-initiated polymerization and rheological properties enable the 3D printing of polymeric RTP hydrogels (Fig. 10d).[46] This fabrication process has achieved micron-scale precision and produced structures with outstanding mechanical performance. Importantly, the printed lattice structures maintained their completeness even after multiple repeated compression cycles (Fig. 10e).

4.2 Bioimaging

The core challenge restricting the sensitivity and accuracy of bioimaging is how to accurately extract the target signal from

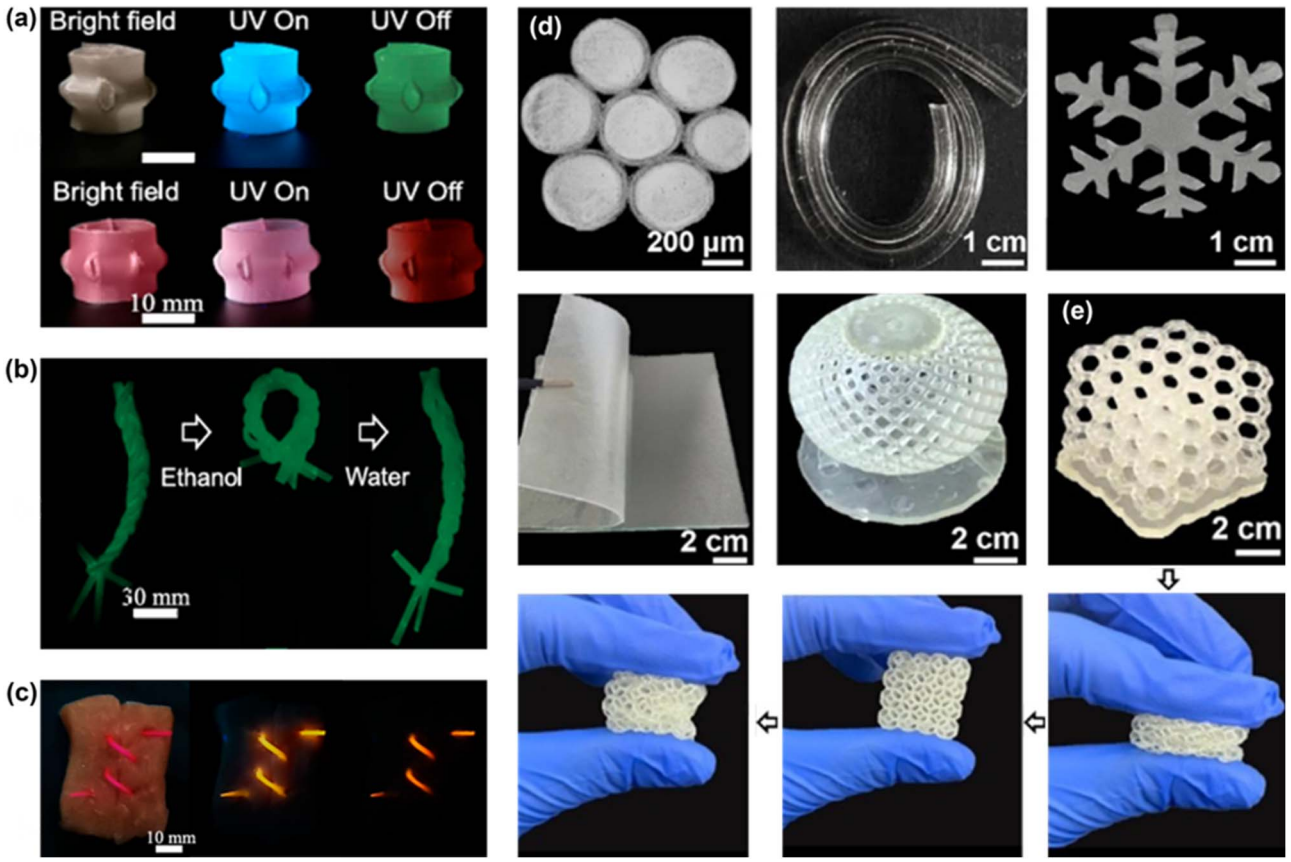

Fig. 10 Applications in 3D printing. (a) Afterglow images of 3D shapes from W-hydrogel and Rhodamine B-doped W-hydrogel. (b) RTP images of textiles made from W-hydrogel threads reversibly treated by ethanol and water. (c) Digital, fluorescent, and afterglow images of pork tissues sutured using RhB@W-hydrogel threads. (d) Photographs illustrating the fibers, snowflake pattern, coating and 3D object prepared by the photopolymerization reaction with BTD-HEA. (e) The lattice maintained its structural integrity after repeated compression.

the complex and auto-fluorescent biological background.[71–75] Certain polymeric RTP hydrogels have ultralong emission lifetimes of milliseconds or even seconds. Researchers can use time-resolved imaging technology to collect long-lived RTP signals after the complete decay of short-lived background fluorescence, thereby achieving ultra-high signal-to-noise ratio imaging. For example, an NIR RTP supramolecular hydrogel was developed based on amphiphilic bromonaphthalimide pyridinium derivatives, nanosheets (LP), AAm and heptamethine cyanine. The hydrogel exhibits low cytotoxicity and good biocompatibility. The NIR emission signal of the RTP hydrogel in HeLa cells was observed by laser scanning microscopy, revealing distinct cellular contours (Fig. 11a).[60] In addition, a NIR RTP hydrogel constructed through supramolecular polymerization using monoalkene-functionalized iodoisoquinolinium derivatives (G′), LP, rhodamine 800 ((Rh800)) and AAm monomers can also achieve similar effects (Fig. 11b).[61]

4.3 Anti-counterfeiting and information encryption

Tunable luminescent performance and the stimulus responsiveness of polymeric RTP hydrogels provide significant application value in anti-counterfeiting and information encryption.[76–79]

Wu and colleagues used the quenching effect of halogen ions on polymeric RTP hydrogels and a fluorescein solution to make hydrogels display different information when the UV lamp was on and off, achieving information encryption. The strategy involves printing the real information “OFF” onto the hydrogel with KI solution. Then, the word “OPEN” is printed onto the hydrogel with fluorescein solution to cover and encrypt the word “OFF”. Upon irradiation under a UV lamp, the area printed with fluorescein had bright-yellow fluorescence, showing the word “OPEN”. Upon removal of the UV lamp, the KI printed area revealed the true information “OFF” due to the difference in phosphorescence intensity between the quenched area and unquenched area (Fig. 12a).[56]

Polymeric RTP hydrogels with excitation wavelength-dependent luminescence provide more possibilities for information encryption. Wang and colleagues obtained a series of excitation wavelength-dependent RTP hydrogels by changing the acid component in the hydrogel (PVA/BIU/PMAc) to alginic acid (Alg), poly(itaconic acid) (PITAc) or poly(maleic acid-*co*-vinyl pyrrolidone) (PMVPAc). The information code was constructed by hydrogel squares with different compositions, which can display various patterns under different wavelengths of excitation. Additionally, several types of hydrogels were used

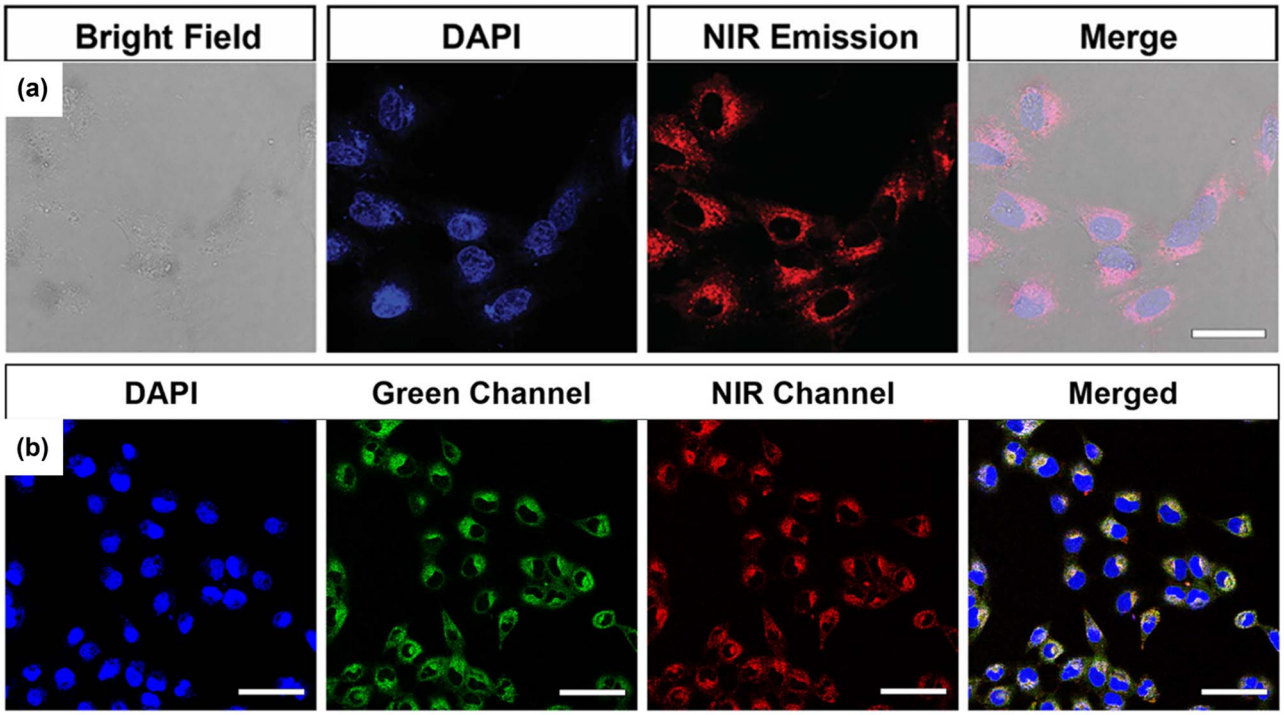

Fig. 11 Applications in bioimaging. (a) Cellular imaging of living HeLa cancer cells stained by G⊂LP@PAAm/IR780. Nuclei stained by 4,6-diamidino-2phenylindole (DAPI, blue) were collected from 420 to 470 nm, while NIR emission was observed from 700 to 800 nm, respectively (scale bar = 25 μm). (b) G⊂LP@PAAm/Rh800. Nuclei stained by DAPI (blue) were acquired from 420 to 470 nm (scale bar = 60 μm).

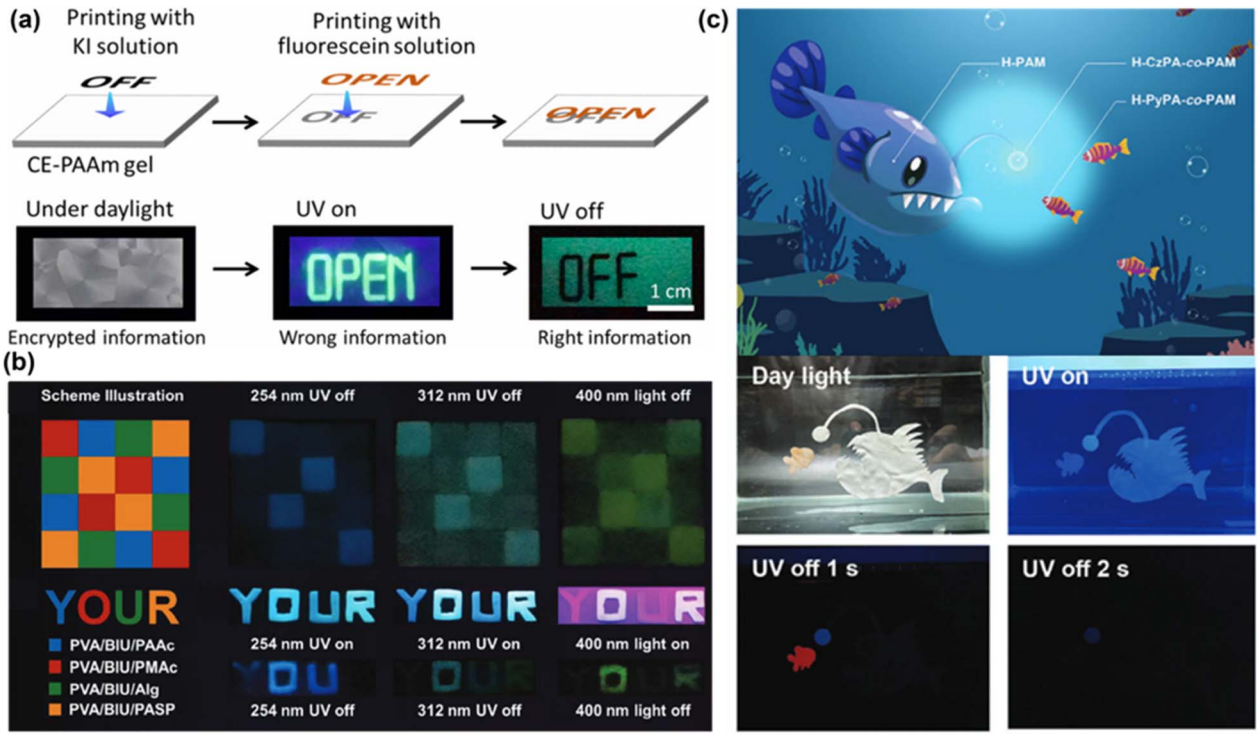

Fig. 12 Applications in anti-counterfeiting encryption (a) Schematic and photographs for the encoding of digital information by printing of KI solution and fluorescein solution on CE-PAAm gel. (b) Schematic illustration and photographs of patterns composed of different hydrogels (PVA/BIU/acid, acid = PASP, PAAc, Alg, PITAc, and PMVPAc) showing different information after excitation under irradiation of different wavelengths. (c) Camouflage of marine animals.

to form the letters "Y," "O," "U," and "R.", respectively. Under excitation of light at 254, 312 or 400 nm, all patterns showed the word "YOUR". However, after turning off the light sources at these respective wavelengths, the patterns of "YOU", "OUR" and "OR" could be observed separately (Fig. 12b).[50]

Furthermore, Lü *et al.* replaced the grafted chromophores in the polymeric RTP hydrogel (H-CzPA-*co*-PAM) with N-1-pyrenyl-2-propenamide (PyPA) to achieve regulation of afterglow color and duration. Also, a conceptual camouflage skin of marine animals was proposed. As shown in Fig. 12c, different polymeric RTP hydrogels were used as multiple functional skins of different deep-sea fishes. After removing the 365 nm UV excitation, the blue lure of the anglerfish attracts other fish (*e.g.*, eyelight fish, marked in red) due to the phototactic of most deep-sea fish preying. The blue lure can also be used for communication between identical species. After removing the 365 nm UV excitation for 2 s, the blue lure was intelligently observed due to the difference in the afterglow time of different polymeric RTP hydrogels, achieving an underwater dynamic temporal information display.[55]

5. Summary and outlook

Polymeric RTP hydrogels are highly sensitive to environmental conditions, particularly water and oxygen, which lead to rapid quenching. The solution to these challenges lies in providing a rigid microenvironment for chromophores in hydrogels to inhibit non-radiative transitions, thereby achieving RTP emission. This review systematically summarizes the construction strategies for polymeric RTP hydrogels: physical doping, chemical grafting, and supramolecular polymerization. Furthermore, the applications of RTP hydrogels in 3D printing, bioimaging, and anti-counterfeiting technology are outlined. Undoubtedly, RTP hydrogels have made significant progress in achieving multifunctionality and stable afterglow, primarily through innovative molecular design and structural design of polymeric hydrogel networks. However, six critical shortcomings remain to be addressed. First, luminous efficiency is lower than that of traditional rigid RTP materials, and the RTP lifetime is relatively short. Second, there are difficulties in the transition from small-scale laboratory preparation to industrial production. Third, RTP performance varies at different positions during 3D printing. Fourth, the design of multi-stimuli-responsive polymeric RTP hydrogels. Fifth, UV excitation is commonly required to achieve RTP emission. Sixth, achieving full-spectrum RTP luminescence remains challenging, especially NIR phosphorescence.

Given these challenges, research should focus on four main areas. First, it is necessary to improve the performance of polymeric RTP hydrogels by developing new chromophores and innovative polymer structure designs. Thus, on the premise of ensuring the advantages of flexibility, efforts should aim to endow polymeric RTP hydrogels with higher luminous efficiency, longer RTP lifetime, and wider spectral emission range. Advances in high-performance RTP hydrogels will drive technological innovations in anti-counterfeiting and information encryption.

Second, the synthetic routes of efficient organic RTP molecules are usually complex, involving multiple reaction steps, with relatively low yields. Gram-scale preparation is feasible, but challenges arise when scaling up to kilogram- or ton-scale production. The key indicators, such as the RTP properties of the final product, may fluctuate between batches, making it difficult to meet the stringent stability requirements for industrial products. The same problem also occurs in 3D printing due to the stability of the prepared RTP polymer ink and the layer-by-layer accumulation process involved in 3D printing. This leads to inconsistent RTP properties in different positions of 3D-printed products, as well as poor stability between batches. Whether it is large-scale production or 3D printing, the future breakthrough direction lies in the deep integration of molecular design, material engineering and process innovation.

Third, the hydrogel network can respond to external stimuli (*e.g.*, pH, temperature, and specific molecules), resulting in changes in volume or conformation, and then manipulating RTP emission provides new opportunities for the design of multi-stimulus-response polymeric RTP hydrogels. The advantage of multi-stimulus-response polymeric RTP hydrogels is that they break the linear mode of "single stimulus–single response", and then turn to the networked mode of "multi-input–intelligent processing–multidimensional output". Thus, "intelligent" materials that can "sense" complex environments and make readable responses are constructed. This provides a new strategy for applications in advanced sensing, information anti-counterfeiting, and other fields.

Fourth, most traditional RTP materials require high-energy UV light excitation, which possesses strong penetration and energy, potentially damaging biological tissues. In contrast, visible light-excited RTP is not affected by these problems, offering vast applications in cutting-edge fields such as bioimaging and intelligent sensing. Owing to the deeper tissue penetration and lower biological background interference of NIR phosphorescence, the development of efficient NIR RTP hydrogels will be a key step in achieving deep, high-resolution *in vivo* imaging, which is extremely challenging but valuable. In addition, there have been relatively few biocompatibility tests conducted on the application of polymeric RTP hydrogels in bioimaging. Related studies on bioimaging should involve comprehensive assessment of biocompatibility, including cytotoxicity and blood compatibility, to ensure that imaging does not cause damage to the organism. In addition, the biodistribution and metabolic pathways of polymeric RTP hydrogels should be studied by *in vivo* imaging systems, and the systemic distribution, organ enrichment and clearance time of polymeric RTP hydrogels (or their degradation products) after injection or implantation should be dynamically monitored to assess their safety in bioimaging applications.

In conclusion, research on polymeric RTP hydrogels has moved from basic material synthesis to the development of function-oriented intelligent devices. It provides innovative solutions to solve challenging problems in biomedicine and information technology.

Author contributions

Tao Chen supervised the manuscript. Wei Lu and Xiaoye Zhang revised the manuscript. Weihao Feng wrote the manuscript. Muqing Si and Kuangzheng Cao contributed to manuscript preparation. All authors revised and finalized the manuscript.

Conflicts of interest

The authors declare no conflicts of interest.

Data availability

No primary research results, software or code have been included and no new data were generated or analyzed as part of this review.

Acknowledgements

This work was supported by Natural Science Foundation of China (22322508), and Zhejiang Provincial Natural Science Foundation of China (LR23E030001).

References

1 Z. Li, X. Ji, H. Xie and B. Z. Tang, *Adv. Mater.*, 2021, **33**, 2100021.
2 S. Cai, Z. Sun, H. Wang, X. Yao, H. Ma, W. Jia, S. Wang, Z. Li, H. Shi, Z. An, Y. Ishida, T. Aida and W. Huang, *J. Am. Chem. Soc.*, 2021, **143**, 16256–16263.
3 X. Ma, J. Wang and H. Tian, *Acc. Chem. Res.*, 2019, **52**, 738–748.
4 J. Guo, C. Yang and Y. Zhao, *Acc. Chem. Res.*, 2022, **55**, 1160–1170.
5 L. Li, J. Zhou, J. Han, D. Liu, M. Qi, J. Xu, G. Yin and T. Chen, *Nat. Commun.*, 2024, **15**, 3846.
6 H. Sun, Q. Zhang, L. Meng, Z. Wang, Y. Fan, M. Mayor, M. Pan and C.-Y. Su, *Chem. Sci.*, 2024, **15**, 8905–8912.
7 H. Shi, W. Yao, W. Ye, H. Ma, W. Huang and Z. An, *Acc. Chem. Res.*, 2022, **55**, 3445–3459.
8 K. Benson, A. Ghimire, A. Pattammattel and C. V. Kumar, *Adv. Funct. Mater.*, 2017, **27**, 1702955.
9 X. Yu, A. A. Ryadun, D. I. Pavlov, T. Y. Guselnikova, A. S. Potapov and V. P. Fedin, *Adv. Mater.*, 2024, **36**, 2311939.
10 Z. Zhang, L. Qian, B. Zhang, C. Ma and G. Zhang, *Angew. Chem., Int. Ed.*, 2024, **63**, e202410335.
11 Q. Dang, Y. Jiang, J. Wang, J. Wang, Q. Zhang, M. Zhang, S. Luo, Y. Xie, K. Pu, Q. Li and Z. Li, *Adv. Mater.*, 2020, **32**, 2006752.
12 Y. Fan, S. Liu, M. Wu, L. Xiao, Y. Fan, M. Han, K. Chang, Y. Zhang, X. Zhen, Q. Li and Z. Li, *Adv. Mater.*, 2022, **34**, 2201280.
13 M. Cui, P. Dai, J. Ding, M. Li, R. Sun, X. Jiang, M. Wu, X. Pang, M. Liu, Q. Zhao, B. Song and Y. He, *Angew. Chem., Int. Ed.*, 2022, **61**, e202200172.
14 F. Xiao, H. Gao, Y. Lei, W. Dai, M. Liu, X. Zheng, Z. Cai, X. Huang, H. Wu and D. Ding, *Nat. Commun.*, 2022, **13**, 186.
15 M. Yao, W. Wei, W. Qiao, Y. Zhang, X. Zhou, Z. Li, H. Peng and X. Xie, *Adv. Mater.*, 2025, 2414894.
16 H. Yang, S. Li, J. Zheng, G. Chen, W. Wang, Y. Miao, N. Zhu, Y. Cong and J. Fu, *Adv. Mater.*, 2023, **35**, 2301300.
17 H. Zhang, B. Zhang, C. Cai, K. Zhang, Y. Wang, Y. Wang, Y. Yang, Y. Wu, X. Ba and R. Hoogenboom, *Nat. Commun.*, 2024, **15**, 2055.
18 W. Luo, L. Chen, G. Yin, C. Yue, S. Xie, J. Zhou, W. Feng, Y. Nie, H. Qiu, F. Li, S. Cai, Y. Li, Z. Cai and T. Chen, *Angew. Chem., Int. Ed.*, 2025, **64**, e202423650.
19 Kenry, C. Chen and B. Liu, *Nat. Commun.*, 2019, **10**, 2111.
20 C. Chen, Z. Chi, K. Chong, A. S. Batsanov, Z. Yang, Z. Mao, Z. Yang and B. Liu, *Nat. Mater.*, 2021, **20**, 175–180.
21 X.-Y. Dai, M. Huo and Y. Liu, *Nat. Rev. Chem.*, 2023, **7**, 854–874.
22 D. Li, Z. Liu, M. Fang, J. Yang, B. Z. Tang and Z. Li, *ACS Nano*, 2023, **17**, 12895–12902.
23 M. Roucan, M. Kielmann, S. J. Connon, S. S. R. Bernhard and M. O. Senge, *Chem. Commun.*, 2018, **54**, 26–29.
24 Q. Yu, Z. Deng, R. Chen, J. Zhang, R. T. K. Kwok, J. W. Y. Lam, J. Sun and B. Z. Tang, *J. Am. Chem. Soc.*, 2025, **147**, 10530–10539.
25 S. Garain, S. N. Ansari, A. A. Kongasseri, B. Chandra Garain, S. K. Pati and S. J. George, *Chem. Sci.*, 2022, **13**, 10011.
26 Y. Deng, P. Chen, X. Yang, N. Li, S. Ma, Z. Huang and S. Lü, *Adv. Mater.*, 2025, **37**, e14693.
27 F. Nie and D. Yan, *Angew. Chem., Int. Ed.*, 2023, **62**, e202302751.
28 B. Zhou, Z. Qi and D. Yan, *Angew. Chem., Int. Ed.*, 2022, **61**, e202208735.
29 Y. N. Ye, K. Cui, W. Hong, X. Li, C. Yu, D. Hourdet, T. Nakajima, T. Kurokawa and J. P. Gong, *Proc. Natl. Acad. Sci. U. S. A*, 2021, **118**, e2014694118.
30 W. Lu, M. Si, X. Le and T. Chen, *Acc. Chem. Res.*, 2022, **55**, 2291–2303.
31 M. Hua, S. Wu, Y. Ma, Y. Zhao, Z. Chen, I. Frenkel, J. Strzalka, H. Zhou, X. Zhu and X. He, *Nature*, 2021, **590**, 594–599.
32 L. Chen, Z. Jin, W. Feng, L. Sun, H. Xu and C. Wang, *Science*, 2024, **383**, 1455–1461.
33 G. Zhang, J. Steck, J. Kim, C. H. Ahn and Z. Suo, *Sci. Adv.*, 2023, **9**, eadh7742.
34 W. Li, X. Wang, Z. Liu, X. Zou, Z. Shen, D. Liu, L. Li, Y. Guo and F. Yan, *Nat. Mater.*, 2024, **23**, 131–138.
35 X. Yao, J. Wang, D. Jiao, Z. Huang, O. Mhirsi, F. Lossada, L. Chen, B. Haehnle, A. J. C. Kuehne, X. Ma, H. Tian and A. Walther, *Adv. Mater.*, 2021, **33**, 2005973.
36 C. Zheng, S. Tao, X. Zhao, C. Kang and B. Yang, *Angew. Chem., Int. Ed.*, 2024, **63**, e202408516.
37 J. Xiao, J. Deng, X. Wang, H. Ho, C. Bai, Y. Bai and H. Wang, *Small*, 2024, **20**, 2405615.
38 Y. Zhang, Y. Su, H. Wu, Z. Wang, C. Wang, Y. Zheng, X. Zheng, L. Gao, Q. Zhou, Y. Yang, X. Chen, C. Yang and Y. Zhao, *J. Am. Chem. Soc.*, 2021, **143**, 13675–13685.
39 S. Tang, S. Jiang, K. Wang, Y. Zhang, L. Yi, J. Hou, L. Qu, Y. Zhao and C. Yang, *Adv. Mater.*, 2025, **37**, 2416397.

40 Z. Man, Z. Lv, Z. Xu, J. He, Q. Liao, Y. Yang, J. Yao and H. Fu, *J. Am. Chem. Soc.*, 2023, **145**, 13392–13399.
41 J. Li, L. Zhang, C. Wu, Z. Huang, S. Li, H. Zhang, Q. Yang, Z. Mao, S. Luo, C. Liu, G. Shi and B. Xu, *Angew. Chem., Int. Ed.*, 2023, **62**, e202217284.
42 T. Zhu, S. Zheng, T. Yang and W. Z. Yuan, *J. Phys. Chem. Lett.*, 2023, **14**, 6451–6458.
43 M. Qi, J. Huang, J. Wei, J. Zhou, D. Liu, L. Li, W. Luo, G. Yin and T. Chen, *Angew. Chem., Int. Ed.*, 2025, **64**, e202501054.
44 X. Huang, Y. Zhang, G. Li, T. Wang, P. Sun, J. Shi, B. Tong, J. Zhi, Z. Li, Z. Cai and Y. Dong, *ChemPhotoChem*, 2024, **9**, e202400315.
45 M. Fang, J. Yang and Z. Li, *Prog. Mater. Sci.*, 2022, **125**, 100914.
46 Y. Cao, D. Wang, Y. Zhang, G. Li, C. Gao, W. Li, X. Chen, X. Chen, P. Sun, Y. Dong, Z. Cai and Z. He, *Angew. Chem., Int. Ed.*, 2024, **63**, e202401331.
47 J. Deng, H. Liu, D. Liu, L. Yu, Y. Bai, W. Xie, T. Li, C. Wang, Y. Lian and H. Wang, *Adv. Funct. Mater.*, 2024, **34**, 2308420.
48 X. Jiang, M. Wu, L. Zhang, J. Wang, M. Cui, J. Wang, X. Pang, B. Song and Y. He, *Anal. Chem.*, 2022, **94**, 7264–7271.
49 Y. Sun, L. Jiang, Y. Chen and Y. Liu, *Chin. Chem. Lett.*, 2024, **35**, 108644.
50 J. Deng, D. Liu, H. Liu, L. Yu, Y. Bai, J. Xiao and H. Wang, *Adv. Funct. Mater.*, 2024, **34**, 2408821.
51 R. Liu, H. Guo, S. Liu, J. Li, S. Li, T. D. James and Z. Chen, *Nat. Commun.*, 2024, **15**, 10588.
52 W. Feng, F. Li, Z. Jiang, C. Yue, G. Yin, N. Zhu, K. Zhang, T. Chen and W. Lu, *Angew. Chem., Int. Ed.*, 2025, **64**, e202505192.
53 H. Chen, X. Ma, S. Wu and H. Tian, *Angew. Chem., Int. Ed.*, 2014, **53**, 14149–14152.
54 H. Chen, L. Xu, X. Ma and H. Tian, *Polym. Chem.*, 2016, **7**, 3989–3992.
55 P. Chen, H. Qie, X. Yang, S. Ma, Z. Wang, N. Li, Y. Deng, F. Bian and S. Lü, *Adv. Funct. Mater.*, 2025, **35**, 2416430.
56 H. Ju, H. Zhang, L. X. Hou, M. Zuo, M. Du, F. Huang, Q. Zheng and Z. L. Wu, *J. Am. Chem. Soc.*, 2023, **145**, 3763–3773.
57 Z. Zhang, H. Ju, H. Zhang, Z. Wang, M. Du, H. Li, F. Huang, Q. Zheng and Z. L. Wu, *Adv. Mater.*, 2025, **37**, 2505444.
58 S. Yu, J. Zhang, X. Chen, X. Wu, X. Zhao, Z. Zhu, J. Zhang, Y. Zuo and C. Zhao, *Adv. Opt. Mater.*, 2024, **12**, 2303330.
59 S. Garain, B. C. Garain, M. Eswaramoorthy, S. K. Pati and S. J. George, *Angew. Chem., Int. Ed.*, 2021, **60**, 19720–19724.
60 Q. Song, Z. Liu, J. Li, Y. Sun, Y. Ge and X. Dai, *Adv. Mater.*, 2024, **36**, 2409983.
61 Q. Song, Z. Liu, X. Bai, Y. Zhang, S. Yang, Y. Ge and X. Dai, *Adv. Opt. Mater.*, 2025, **13**, 2500624.
62 X. Sun, H. Yang, W. Zhang, S. Zhang, J. Hu, M. Liu, X. Zeng, Q. Li, C. Redshaw, Z. Tao and X. Xiao, *ACS Appl. Mater. Interfaces*, 2023, **15**, 4668–4676.
63 W. Zhao, Z. He and B. Z. Tang, *Nat. Rev. Mater.*, 2020, **5**, 869–885.
64 G. Baryshnikov, B. Minaev and H. Ågren, *Chem. Rev.*, 2017, **117**, 6500–6537.
65 H. Sun, M. He, G. V. Baryshnikov, B. Wu, R. R. Valiev, S. Shen, M. Zhang, X. Xu, Z. Li, G. Liu, H. Ågren and L. Zhu, *Angew. Chem., Int. Ed.*, 2024, **63**, e202318159.
66 G. Yin, W. Lu, J. Huang, R. Li, D. Liu, L. Li, R. Zhou, G. Huo and T. Chen, *Aggregate*, 2023, **4**, e344.
67 Z. Xie, P. Sun, Z. Wang, H. Li, L. Yu, D. Sun, M. Chen, Y. Bi, X. Xin and J. Hao, *Angew. Chem., Int. Ed.*, 2020, **59**, 9922–9927.
68 J. Chen, F. Lin, D. Guo, T. Tang, Y. Miao, Y. Wu, W. Zhai, H. Huang, Z. Chi, Y. Chen and Z. Yang, *Adv. Mater.*, 2024, **36**, 2409642.
69 H. Sun, Y. Xiao, Y. He, X. Wei, J. Zou, Y. Luo, Y. Wu, J. Zhao, V. K.-M. Au and T. Yu, *Chem. Sci.*, 2025, **16**, 5299–5309.
70 P. Wu, P. Li, M. Chen, J. Rao, G. Chen, J. Bian, B. Lue and F. Peng, *Adv. Mater.*, 2024, **36**, 2402666.
71 J. Zhu, L. Luo, M. Gu, Y. Chen, L. Wang, M. Li, X. Chen and X. Peng, *CCS Chem.*, 2025, **7**, 1552–1566.
72 J. Yuan, H. Yang, W. Huang, S. Liu, H. Zhang, X. Zhang and X. Peng, *Chem. Soc. Rev.*, 2025, **54**, 341–366.
73 T. Xiong, Y. Chen, Q. Peng, M. Li, S. Lu, X. Chen, J. Fan, L. Wang and X. Peng, *J. Am. Chem. Soc.*, 2024, **146**, 24158–24166.
74 H. Gao, T. Zhang, Y. Lei, D. Jiao, B. Yu, W. Z. Yuan, J. Ji, Q. Jin and D. Ding, *Angew. Chem., Int. Ed.*, 2024, **63**, e202406651.
75 L. Li, D. Liu, J. Zhou, M. Qi, G. Yin and T. Chen, *Mater. Horiz.*, 2024, **11**, 5895–5913.
76 Y. Shen, X. Le, Y. Wu and T. Chen, *Chem. Soc. Rev.*, 2024, **53**, 606–623.
77 J. Xiang, Y. Shi, J. Jiang, J. Yan, S. Xiao, H. Lin and T. Yi, *Adv. Opt. Mater.*, 2024, **12**, 2302671.
78 J. Wei, Y. Xiao, J. Luo, Z. He, J. Chen, Q. Peng and D. Kuang, *Chem. Sci.*, 2025, **16**, 7239–7248.
79 J. Xue, Z. Qi, D. Yan, G. Yang and Y. Wang, *Angew. Chem., Int. Ed.*, 2025, **64**, e202501951.